HYDROLOGICAL PROCESSES
Hydrol. Process. **20**, 3897–3913 (2006)
Published online 8 June 2006 in Wiley InterScience (www.interscience.wiley.com). DOI: 10.1002/hyp.6163

Field determination of the spatial variation of resistance to flow along a steep Alpine stream

S. Orlandini,[1]* C. Boaretti,[2] V. Guidi[3] and G. Sfondrini[4]

[1] *Dipartimento di Scienze Agrarie, Università degli Studi di Modena e Reggio Emilia, Via Kennedy 17, I-42100 Reggio Emilia, Italy*
[2] *Stazione Valchiavenna per lo Studio dell'Ambiente Alpino, Via Cappuccini, I-23022 Chiavenna, Italy*
[3] *Dipartimento di Fisica, Università degli Studi di Ferrara, Via Saragat 7, I-44100 Ferrara, Italy*
[4] *Dipartimento di Scienze della Terra, Università degli Studi di Milano, Via Mangiagalli 34, I-20133 Milan, Italy*

Abstract:

Accurate field data have been collected along the Febbraro River (central Italian Alps) during quasi-steady, low-flow conditions to investigate the spatial variations of hydraulic and geomorphologic quantities potentially affecting resistance to flow. Detailed uncertainty analysis and weighted least-squares fitting of simple power function relationships to field-derived data are carried out to identify possible interdependencies between observed variables. Mean flow velocity is found to depend on water-surface slope, bed material particle size, and upstream drainage area, whereas its dependence on hydraulic depth appears less susceptible to quantification. Upstream drainage area is found to explain the variations of hydraulic depth, water-surface slope, Gauckler–Strickler conductance coefficient, and (although less significantly) flow discharge. Specifically, a highly significant positive dependence of the Gauckler–Strickler conductance coefficient on the upstream drainage area is found to exist, although anomalies in the variations of hydraulic depth and flow discharge are observed along the stream. The combined use of uncertainty analysis, hydraulic equations, and geomorphological relationships allows a possible characterization of resistance to flow along a steep Alpine stream and, perhaps more importantly, provides useful guidelines for future investigative efforts. Copyright © 2006 John Wiley & Sons, Ltd.

KEY WORDS Alpine streams; stream flow; resistance coefficients; field data; uncertainty analysis

INTRODUCTION

In steep mountain streams, when mean flow depth is of comparable magnitude to bed material particle size, the resistance to flow can hardly be described using the hydraulics developed for gravel bed rivers and low-gradient channels (Bathurst, 1993; Wohl, 2000). Hydraulic formulations proposed in the literature for steep mountain streams generally express resistance coefficients as (also) being functions of channel bed slope (Smart and Jaeggi, 1983; Jarrett, 1984). Using an apparently different approach, geomorphological fluvial relationships employ a reference discharge of assigned frequency (usually at the bankfull stage) to explain the downstream variations of flow characteristics and resistance coefficients (Leopold and Maddock, 1953; Leopold *et al.*, 1964).

Despite the many past attempts to characterize the hydraulics of mountain streams, as reported by Wohl (2000: 82), there is not at present a well-tested, consistently accurate equation for calculating resistance coefficients of mountain rivers. Considerable fieldwork is required to provide reliable explicative and predictive models of the hydraulics of mountain streams (during flooding conditions) and of related processes, such as sediment transport, bedform and channel morphology, and longitudinal profile development (Wohl, 2000: 232). In addition, accurate characterizations of the variation of mean flow velocity and resistance to flow

* Correspondence to: S. Orlandini, Dipartimento di Scienze Agrarie, Università degli Studi di Modena e Reggio Emilia, Via Kennedy 17, I-42100 Reggio Emilia, Italy. E-mail: stefano.orlandini@unimore.it

Received 7 March 2005
Accepted 16 September 2005

along mountain streams (during low-flow conditions) appear critical to understanding the links between land use changes and physical stream habitat responses so that management and restoration strategies can be guided (e.g. Jacobson *et al.*, 2001: 7).

To understand and predict the variation of resistance to flow across a complex channel network, hydraulic and geomorphological relationships were combined by Orlandini and Rosso (1998) and Orlandini (2002). The methodology explored in these studies was to determine in the field the downstream fluvial relationships for relevant hydraulic quantities during quasi-steady (low) flow conditions (when surveys are practicable), and to combine these downstream relationships with at-a-station relationships for estimating the temporal variations of the same hydraulic quantities during flooding conditions (when surveys are relatively less practicable). This paper contributes to develop and test the first phase of this methodology by focusing the attention on the field determination of the spatial variation of flow characteristics along a steep Alpine stream.

BACKGROUND

Two flow resistance formulations commonly used in channel flow hydraulics are the Darcy–Weisbach (DW) equation

$$U = \left(\frac{8gY_{\mathrm{m}}S_{\mathrm{f}}}{f}\right)^{1/2} \tag{1}$$

where U is the mean flow velocity, g is the acceleration due to gravity, Y_{m} is the hydraulic depth (mean flow depth), S_{f} is the friction slope and f is the DW resistance coefficient, and the Gauckler–Manning–Strickler (GMS) equation

$$U = k_{\mathrm{S}}Y_{\mathrm{m}}^{2/3}S_{\mathrm{f}}^{1/2} \tag{2}$$

where k_{S} is the Gauckler–Strickler (GS) conductance coefficient. This is the equation best known in the English literature as the Manning equation, k_{S} being equal to $1/n$, where n is the Manning resistance coefficient (Williams, 1970; Hager, 2001). For flows in boulder-bed rivers with relative submergences $Y_{\mathrm{m}}/D_{84} \leq 10$, D_{84} being the bed material particle size for which 84% of the material is finer, and channel bed slope $S_{\mathrm{b}} = 0{\cdot}004–0{\cdot}040$, the relationship

$$\left(\frac{8}{f}\right)^{1/2} = 5{\cdot}62\log\left(\frac{Y_{\mathrm{m}}}{D_{84}}\right) + 4 \tag{3}$$

has been proposed by Graf *et al.* (1983) and Bathurst (1985). For flows in steep pool–fall streams with $Y_{\mathrm{m}}/D_{90} \leq 10$, D_{90} being the bed material particle size for which 90% of the material is finer, and $S_{\mathrm{b}} = 0{\cdot}040–0{\cdot}200$, the relationship

$$\left(\frac{8}{f}\right)^{1/2} = 5{\cdot}75\left[1 - \exp\left(-\frac{0{\cdot}05Y_{\mathrm{m}}}{D_{90}S_{\mathrm{b}}^{1/2}}\right)\right]^{1/2}\log\left(\frac{8{\cdot}2Y_{\mathrm{m}}}{D_{90}}\right) \tag{4}$$

has been proposed by Smart and Jaeggi (1983). Jarrett (1984) suggested estimating the GS conductance coefficient in steep mountain streams with slope up to 0·09 and low relative submergences using the relationship

$$k_{\mathrm{S}} = 3{\cdot}125Y_{\mathrm{m}}^{0{\cdot}16}S_{\mathrm{f}}^{-0{\cdot}38} \tag{5}$$

Equations (3)–(5) are assumed in this study to constitute the best available estimators for DW resistance coefficients and GS conductance coefficients of mountain rivers based on local measurements of channel and flow characteristics.

A more general formulation was recently proposed by Orlandini (2002) to describe the spatial variation of resistance to flow across a complex channel network. This formulation combines the GMS Equation (2) and geomorphological fluvial relationships of the upstream drainage area A contributing to each fluvial section for U, Y_m, S_f, and k_S, namely

$$U = kA^m \tag{6}$$

$$Y_m = cA^f \tag{7}$$

$$S_f = tA^z \tag{8}$$

$$k_S = rA^y \tag{9}$$

where coefficients (k, c, t, and r) and exponents (m, f, z, and y) need to be estimated on the basis of field observations collected along the fluvial system considered. (Note that the same symbol f is used in this paper to denote both the DW resistance coefficient and the exponent in Equation (7).) These relationships can be derived by combining downstream fluvial relationships proposed by Leopold and Maddock (1953) and the relationship

$$Q = uA^w \tag{10}$$

where u is a coefficient and w is an exponent, which expresses the variation of flow discharge Q with upstream drainage area A. It is acknowledged here that the most meaningful discharge for any discussion of channel morphology is the one that forms or maintains the channel, and that this effective discharge is commonly approximated by bankfull discharge. However, field data collected during quasi-steady, low-flow conditions are employed in this study to investigate the spatial variations of flow characteristics under these complex circumstances and to explore the possibility to surrogate bankfull discharge and related flow characteristics with more easily observable field data.

The formulation proposed by Orlandini (2002) is essentially based on the functional relationship

$$k_S(A) = \frac{U(A)}{Y_m(A)^{2/3} S_f(A)^{1/2}} \tag{11}$$

The variations of U, Y_m, and S_f with A are approximated by fitting observed data to Equations (6), (7), and (8) respectively. In particular, values of water-surface slope S_w are used to estimate the variation of S_f with A. The variation of k_S with A is reproduced either by computing k_S using measured values in Equation (11) and fitting the resulting values using Equation (9), or by applying relationships $r = k/(c^{2/3}t^{1/2})$ and $y = m - 2/3f - 1/2z$ implied by a consistent combination of the GMS Equation (2) and estimated fluvial relationships in Equations (6)–(9) at different sites along the fluvial systems (Leopold *et al.*, 1964: 269).

The practical utility of the formulation proposed by Orlandini (2002) is that it enables hydrologists and geomorphologists to parameterize the GMS Equation (2) at any location along a complex mountain stream. By using the GMS Equation (2) with values of k_S given by the estimated fluvial relationship in Equation (9), values of Y_m given by the estimated fluvial relationship in Equation (7), and observed values of S_w (for S_f), predictions of the mean flow velocity U can ultimately be provided using A and S_w as explicative variables. These variables can readily be derived from terrain analysis for any location along the stream. As detailed in Orlandini (2002), the non-local mapping between the variations of S_f and S_w with A is the central point of the proposed formulation, since it implies (although in an approximate manner) the balance between energy globally provided to the flows by gravitational forces and energy globally dissipated in the flows by frictional forces. This balance is not necessarily ensured by estimating values of k_S using equations reported in the literature or methodologies based on the visual comparison between the fluvial system considered and other systems surveyed (Barnes, 1967; Hicks and Mason, 1991).

STUDY AREA AND FIELD CAMPAIGN

This study draws upon detailed field data collected in summer 2002 along the mainstem of the Febbraro catchment (central Italian Alps). A map of the Febbraro catchment is shown in Figure 1 and field-derived

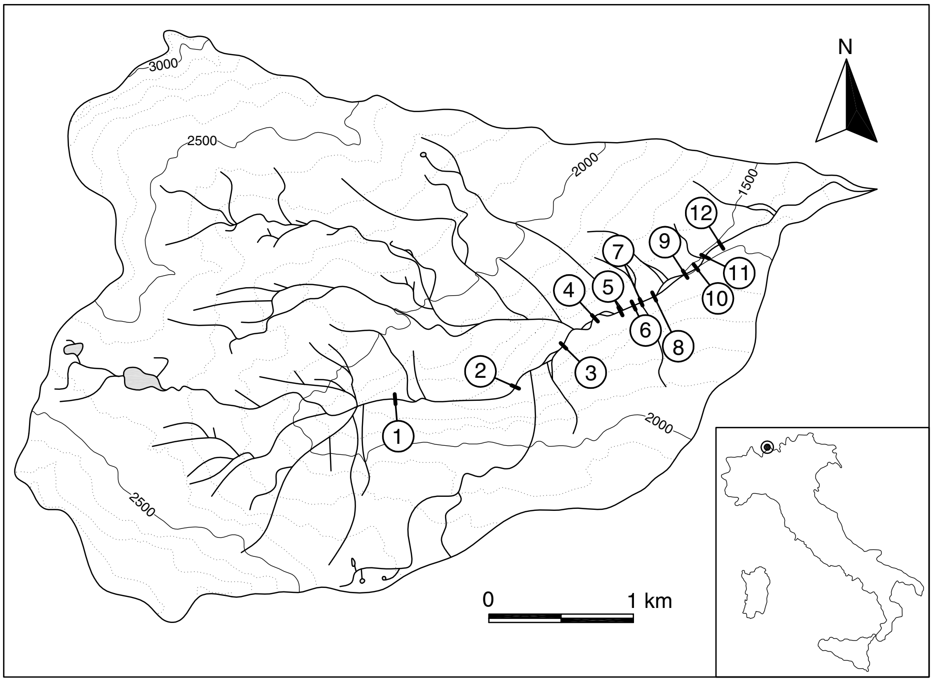

Figure 1. Map of the Febbraro catchment (central Italian Alps) showing the stream channel cross-sections surveyed (Table I)

Table I. Field-derived data used for the description of resistance to flow along the Febbraro River[a]

XS	A (km^2)	D_{84} (m)	D_{90} (m)	S_b	S_w	W (m)	Y_m (m)	U (m s^{-1})	Q (m^3 s^{-1})	k_S (m$^{1/3}$ s^{-1})
1	4·071	0·963	1·224	0·172	0·166	1·50	0·171	0·067	0·017	0·534
2	5·015	0·590	0·848	0·168	0·181	4·60	0·368	0·186	0·315	0·853
3	6·387	0·525	0·724	0·069	0·071	4·20	0·345	0·262	0·380	2·006
4	11·074	0·306	0·449	0·047	0·047	7·25	0·290	0·334	0·702	3·501
5	11·397	0·891	1·062	0·048	0·054	6·05	0·203	0·205	0·252	2·558
6	12·158	0·575	0·719	0·053	0·049	3·30	0·331	0·344	0·376	3·240
7	12·340	0·508	0·657	0·041	0·041	5·00	0·289	0·282	0·408	3·206
8	12·518	0·254	0·382	0·052	0·056	6·35	0·228	0·510	0·739	5·776
9	13·185	0·321	0·400	0·045	0·047	6·25	0·254	0·462	0·733	5·314
10	13·309	0·301	0·355	0·043	0·047	5·95	0·206	0·446	0·547	5·910
11	13·614	0·423	0·613	0·048	0·056	8·80	0·233	0·378	0·775	4·243
12	13·731	0·249	0·311	0·029	0·028	7·30	0·234	0·445	0·761	7·033

[a] Field measurements at stream channel cross-sections 1–5, 7, and 10 were collected during the period 18–24 July 2002, whereas field measurements at stream channel cross-sections 6, 8, 9, 11, and 12 were collected during the period 2–6 September 2002. Although flow conditions were observed to be slightly higher in the second period, all the data collected in summer 2002 can be reasonably used to represent the same quasi-steady flow conditions.

data are reported in Table I. The area of the Febbraro catchment is about 15 km^2. The terrain is mountainous, with elevation range above sea level between 1250 and 3158 m. The catchment is in a near natural condition, with no human settlements. Erosion can be observed throughout the catchment, with gullying at the stream heads and extensive areas of sheet and scree erosion on hillsides. Alluvial and bedrock channels comprise a complex drainage network. Channel properties and flow characteristics were measured at 12 cross-sections (XS in Table I) along the mainstem (Figure 1). Bed material particle sizes were determined using the Wolman (1954) method. At least 100 individual pebbles were picked up from the stream bed around each cross-section. The maximum size of boulders observed along the stream was estimated, and this size was used as spacing between sampling points along the transversal coordinate as well as spacing between transects along the longitudinal coordinate. It is specified here that pebbles were picked up from the entire stream bed, not just from the wetted stream bed, to obtain a practically sufficient sample size also for cross-sections characterized by small water-surface widths (Table I). For instance, sampling points along 20 transects with length of about 5 m and spacing of about 1 m were considered for XS 1, resulting in a sampling area of about 100 m^2.

Channel and water-surface slopes were determined from detailed topographic surveys. Elevation differences were measured using a precision level and a 5 m vertical stadia rod. Distances were determined using an electronic distance measurement system. Measurements were made over fixed distances centred on each cross-section, over a channel unit identified in the field in such a way to include at least two step–pool structures. This will be discussed in the 'Analysis of uncertainties in field-derived data' section, when addressing the uncertainties associated with slope measurements. It is acknowledged here that observational problems connected to the determination of water-surface slope can be mitigated by considering channel segments as elementary observational units instead of individual cross-sections (Barnes, 1967; Hicks and Mason, 1991; MacFarlane and Wohl, 2003). However, this would imply averaging all the observed quantities over channel segments, and thus a loss of detail in the description of channel and flow variabilities. Therefore, individual cross-sections are used in this paper as elementary observational units, and uncertainties arising from this methodology are evaluated by performing a detailed analysis ('Analysis of uncertainties in field-derived data' section). In this paper, local measurements of water-surface slope S_w are substituted for both friction slope S_f and channel bed slope S_b in Equations (1), (2), (4), and (5), since no significant differences between S_b and S_w were observed along the Febbraro River (Table I). Cross-sectional geometries, velocities, and discharges were evaluated through the velocity–area method as described in Nolan and Shields (2000). Values of k_S obtained using measured values in Equation (11) are reported in Table I. Drainage areas contributing to each cross-section were determined from mapping onto 1 : 10 000-scale topographic maps.

A downstream decrease of flow discharge between cross-sections 4 and 5 was clearly noted during the field campaign of summer 2002. Measurements were repeated at cross-sections 4, 5, and 6, and accurate monitoring of water-surface levels was carried out to evaluate possible temporal variations of flows. These variations were not observed. No important rainfall events occurred when measurements at cross-sections 3, 4, and 5 were made. No melt water contributions formed during the field campaign of summer 2002, since snow was not present in the upstream contributing catchments. Uncertainties in field-derived data (calculated in the 'Analysis of uncertainties in field-derived data' section) do not bring significant indetermination into the observed variations. From field observation and data analysis it may be concluded that the anomalous downstream decreases of flow discharge along the Febbraro River are likely to be connected to localized contributions to surface flows released by tributaries and reinfiltration flows along the fluvial system. Specifically, an important left tributary joins the mainstem of the Febbraro catchment just upstream of cross-section 4, forming a high cascade before the junction. This may cause subsurface water flowing through the bed of the tributary to rise before the cascade, to constitute a special contribution to surface flow around cross-section 4, and to reinfiltrate rapidly downstream of cross-section 4 as a consequence of the high hydraulic conductivity of bed material.

ANALYSIS OF UNCERTAINTIES IN FIELD-DERIVED DATA

A detailed analysis of uncertainties has been carried out to assess the margin of indetermination affecting field-derived data. Results are reported in Table II. This section may be skipped without loss of continuity by readers who are not interested in the calculation of uncertainty bars for field-derived data.

Table II. Uncertainties in the field-derived data reported in Table I

XS	δA (km^2)	δD_{84} (m)	δD_{90} (m)	δS_b	δS_w	δW (m)	δY_m (m)	δU (m s^{-1})	δQ (m^3 s^{-1})	δk_S (m$^{1/3}$ s^{-1})
1	0·090	0·095	0·118	0·026	0·025	0·02	0·048	0·016	0·003	0·199
2	0·100	0·055	0·087	0·028	0·030	0·05	0·006	0·022	0·029	0·193
3	0·113	0·052	0·073	0·016	0·017	0·04	0·006	0·032	0·037	0·529
4	0·148	0·029	0·047	0·011	0·011	0·07	0·006	0·049	0·074	1·030
5	0·150	0·089	0·107	0·009	0·010	0·06	0·006	0·025	0·021	0·625
6	0·155	0·055	0·075	0·008	0·007	0·03	0·012	0·052	0·043	0·832
7	0·156	0·052	0·062	0·005	0·005	0·05	0·006	0·038	0·043	0·704
8	0·157	0·024	0·039	0·004	0·004	0·06	0·006	0·064	0·065	1·126
9	0·161	0·030	0·041	0·003	0·003	0·06	0·005	0·048	0·053	0·881
10	0·162	0·030	0·036	0·002	0·003	0·06	0·008	0·071	0·060	1·330
11	0·164	0·040	0·064	0·002	0·002	0·09	0·005	0·047	0·064	0·753
12	0·165	0·023	0·032	0·002	0·002	0·07	0·006	0·065	0·076	1·483

For each cross-section, flow discharge Q is determined through the velocity–area method described by Nolan and Shields (2000). A marked line is stretched across the stream and a suitable number N of intervals along the line are selected to describe the cross-sectional shape and flow variability. At the ith interval ($i = 1, \ldots, N$), the interval length Δw_i is measured on the marked line, the depth of water y_i is measured with a graduated rod, and flow velocities are measured using a current meter at up to three points along the vertical profile (0·2, 0·6, and 0·8 depth). Flow discharge is computed as $Q = \sum_{i=1}^{N} Q_i$, where $Q_i = \Delta w_i y_i \overline{u}_i$ and $\overline{u}_i$ is the average of flow velocity measurements along the vertical profile. By assuming that the systematic (or bias) errors affecting the measurements are negligible and that no relationship would affect the statistical independence of the measurements, the fractional uncertainty in the observed flow discharge Q_i can be expressed as

$$\frac{\delta Q_i}{Q_i} = \frac{\delta \Delta w_i}{\Delta w_i} + \frac{\delta y_i}{y_i} + \frac{\delta \overline{u}_i}{\overline{u}_i} \tag{12}$$

Here, the fractional uncertainty in Q_i is the ordinary sum of the original fractional uncertainties in Δw_i, y_i, and $\overline{u}_i$. Equation (12) provides an upper bound for $\delta Q_i / Q_i$ and is applied, since no specific information about the nature of random variables y_i and $\overline{u}_i$ is known (Taylor, 1997).

The elemental length Δw_i is a directly measured physical quantity and can, therefore, be represented by a normally distributed random variable (i.e. a constant value plus a normally distributed random measurement error). Typical values for Δw_i and its (root-mean-square, RMS) uncertainty $\delta \Delta w_i$ are 0·200 m and 0·005 m respectively. Conversely, owing to the geometrical complexity of the channel bed, the flow depth y_i cannot be considered as being a properly defined physical quantity, and thus it does not admit a true value (Taylor, 1997: 130). However, it is reasonable to assume that the range of y_i is no larger than the interval Δw_i, such that y_i can be represented by a uniformly distributed random variable centred on the measured value and ranging within $\pm \Delta w_i / 2$. The RMS of such a distribution can therefore be expressed by $\delta y_i = \Delta w_i / \sqrt{12}$, as a representation of the uncertainty over y_i. Typical values for y_i and its (RMS) uncertainty δy_i are 0·30 m and 0·04 m respectively. Likewise (though for different reasons), flow velocity $\overline{u}_i$ should not be considered as being a properly defined physical quantity because of the hydraulic complexity of the velocity profile. A uniformly distributed random variable is, therefore, used to represent $\overline{u}_i$. This random variable is centred on the value obtained from measurements and its range is conservatively assumed to be equal to the maximum excursion of the recorded determinations of flow velocity along the vertical profile. Typical values for $\overline{u}_i$ and its (RMS) uncertainty $\delta \overline{u}_i$ are 0·32 m s^{-1} and 0·08 m s^{-1} respectively.

Under the assumption that flow discharges Q_i ($i = 1, \ldots, N$) are statistically independent and their uncertainties δQ_i have comparable magnitudes, then the central limit theorem claims that the variable

$Q = \sum_{i=1}^{N} Q_i$ tends to assume a normal distribution with average $N\langle Q_i \rangle$ and standard deviation approximately given by $\sqrt{N}\langle \delta Q_i \rangle$ in the limit that N approaches infinity. Hence, the fractional uncertainty of the cross-sectional flow discharge Q can be approximated by

$$\frac{\delta Q}{Q} = \frac{1}{\sqrt{N}} \left\langle \frac{\delta Q_i}{Q_i} \right\rangle \tag{13}$$

where $\langle \delta Q_i / Q_i \rangle$ is the average fractional uncertainty over the N intervals into which the section is partitioned. Over the 12 cross-sections surveyed, N ranges from 8 to 33, $\langle \delta Q_i / Q_i \rangle$ ranges from 0·392 to 0·528, and $\delta Q / Q$ ranges from 0·073 to 0·170. Uncertainty bars for the observed values of Q are reported in Table II and shown in Figure 3d. Analogously, the fractional uncertainty in the cross-sectional flow area $\Omega = \sum_{i=1}^{N} \Omega_i$, where $\Omega_i = \Delta w_i y_i$, can be approximated by

$$\frac{\delta \Omega}{\Omega} = \frac{1}{\sqrt{N}} \left\langle \frac{\delta \Omega_i}{\Omega_i} \right\rangle \tag{14}$$

where $\langle \delta \Omega_i / \Omega_i \rangle$ is the average fractional uncertainty over the N intervals into which the section is partitioned. Over the 12 cross-sections surveyed, $\langle \delta \Omega_i / \Omega_i \rangle$ ranges from 0·115 to 0·241 and $\delta \Omega / \Omega$ ranges from 0·026 to 0·072.

It is acknowledged here that the assumption of statistical independence between elemental flow discharges Q_i $(i = 1, \ldots, N)$ mentioned above is not valid for any channel flow. For flows occurring in regular, low-gradient channels there are sufficient data and theoretical understanding to enable the velocity distribution in a cross-section to be predicted with reasonable accuracy, and this makes the above assumption hardly supportable and, what is more, poorly useful. However, for flows occurring in steep mountain streams, accurate predictions of flow velocity distribution in a cross-section can hardly be provided due to the high inherent complexity of channel morphology, and this makes the above assumption more palatable and, what is more, more useful. In this study, the assumption of statistical independence between elemental flow discharges is believed to be sufficiently realistic, since highly variable channel flows are considered and sampling lengths Δw_i $(i = 1, \ldots, N)$ of comparable magnitude to channel heterogeneity scales are selected during the field campaign. Future work may be carried out to provide a more accurate evaluation of the characteristic sampling length above which the assumption discussed here is sensible.

On the basis of the estimates provided by Equations (13) and (14), the fractional uncertainty in mean flow velocity $U = Q/\Omega$ at a given cross-section can be evaluated as

$$\frac{\delta U}{U} = \frac{\delta Q}{Q} + \frac{\delta \Omega}{\Omega} \tag{15}$$

This equation is likely to overestimate the fractional uncertainty $\delta U / U$ because it does not account for possible compensation of the uncertainties in the ratio of the two dependent quantities Q and Ω. However, as one contribution $(\delta Q / Q)$ is dominant with respect to the other $(\delta \Omega / \Omega)$, Equation (15) appears sufficiently accurate. Over the 12 cross-sections surveyed, $\delta U / U$ ranges from 0·056 to 0·676. Uncertainty bars for the measured values of U are reported in Table II and shown in Figures 2 and 4.

The fractional uncertainty in mean flow depth $Y_{\mathrm{m}} = \Omega / W$, where W is the water-surface width, can be estimated on the strength of the statistical independence between Ω and W through the equation

$$\frac{\delta Y_{\mathrm{m}}}{Y_{\mathrm{m}}} = \sqrt{\left(\frac{\delta \Omega}{\Omega}\right)^2 + \left(\frac{\delta W}{W}\right)^2} \tag{16}$$

Here, the fractional uncertainty in Y_{m} is the quadratic sum of the original fractional uncertainties in Ω and W. Equation (16) is applied as Ω and W can reasonably be assumed independent random variables at a given cross-section. Ω is the sum of a large number of independent random variables and (by virtue of the central limit theorem) tends, therefore, to assume a normal distribution. W is a direct measure of a well-defined physical quantity and may, therefore, be regarded as being normally distributed. Under these circumstances, fractional uncertainties in Ω and W can be added in quadrature to provide the fractional uncertainty in Y_m (Taylor, 1997: 61). Over the 12 cross-sections surveyed, $\delta W/W$ is estimated to have a constant value of 0·010, and $\delta Y_m/Y_m$ ranges from 0·015 to 0·280. Uncertainty bars for the observed values of Y_m are reported in Table II and shown in Figures 2a and 3a. It is noted here that uncertainty bars on Y_m do not represent the longitudinal variability of Y_m along the channel, which is normally very high when mountain streams and low-flow conditions are considered.

The water-surface slope S_w at a given cross-section is not a properly defined physical quantity, as its determination depends strongly on the locations of the upstream and downstream sections selected for its evaluation. The fractional uncertainty in S_w is mostly determined by the complexity of the step–pool channel profile rather than by the use of a level, stadia rod and electronic distance-measuring system. Therefore, it appears reasonable to assume that a uniformly distributed random variable represents S_w. This random variable is centred on the measured value and its range is conservatively assumed to be equal to half the ratio step height to the length of step–pool unit (i.e. step crest to step crest) in the fluvial system around the cross-section surveyed. This range appears reasonable, since the lengths of the channel units over which S_w has been measured were selected in such a way that at least two step–pool structures were included. Over the 12 cross-sections surveyed, $\delta S_w/S_w$ ranges from 0·036 to 0·236. Uncertainty bars for the measured values of S_w are reported in Table II and shown Figures 2b and 3b.

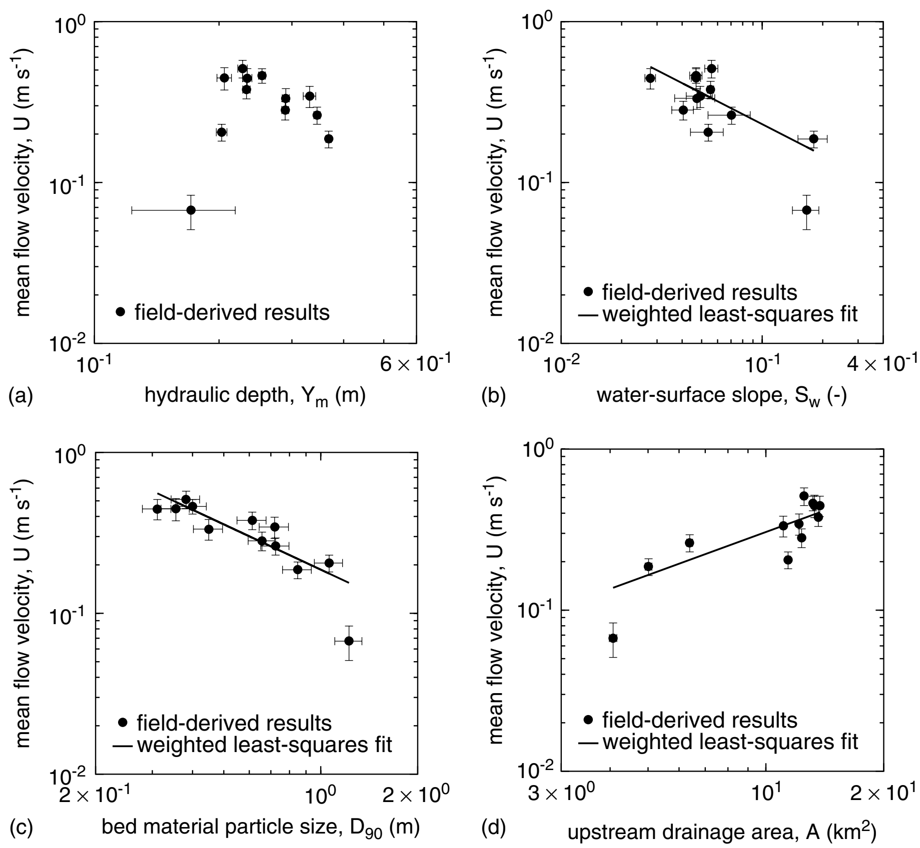

Figure 2. Dependence of mean flow velocity on relevant channel properties and flow characteristics (Table III)

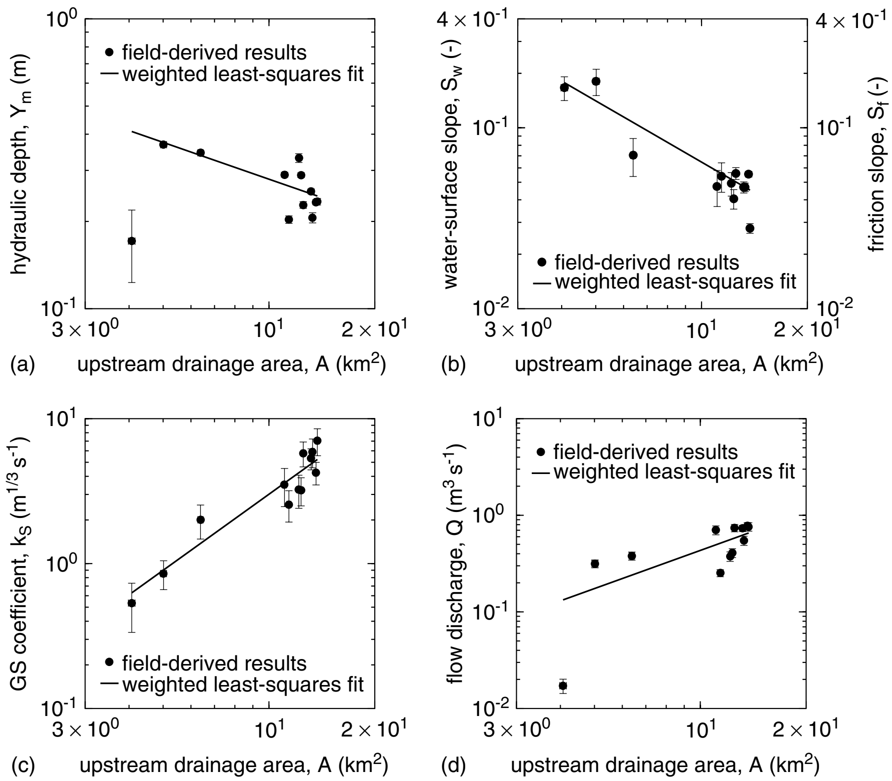

Figure 3. Variations of relevant channel properties and flow characteristics with the upstream drainage area (Table IV). Field-derived values of k_S in plot (c) are obtained using measured values of U, Y_m, and S_w (for S_f) in Equation (11)

The fractional uncertainty in the bed material particle size D_{90} is estimated by assuming that: (1) the repeatability of the sampling procedure proposed by Wolman (1954) implies the existence of a random variable that represents the bed material particle size D in the fluvial system around the cross-section surveyed; (2) a large (greater than 100) number of bed material particles are sampled; and (3) a large (greater than 18) number of classes are used to determine the cumulative frequency curve for the bed material particle size D. Under these assumptions, the number of elements ν_j belonging to the jth equivalence class for D is represented by a Poisson random variable, the best estimate of the number of elements falling in the jth class is the observed value ν_j, and the related uncertainty can be estimated as being $\sqrt{\nu_j}$ (Taylor, 1997: 249). Since the sum of Poisson random variables is still a Poisson random variable, the number of elements that falls in the first j classes is given by $\sum_{k=1}^{j} \nu_k$ and the related uncertainty is $\sqrt{\sum_{k=1}^{j} \nu_k}$. By assuming that the fractional uncertainty in D_{90} is comparable with the uncertainty in the number of elements $N_{D_{90}}$, whose size D is smaller than D_{90}, it holds that

$$\frac{\delta D_{90}}{D_{90}} = \frac{\sqrt{N_{D_{90}}}}{N_{D_{90}}} \tag{17}$$

Over the 12 cross-sections surveyed, $N_{D_{90}}$ ranges from 92 to 113 and $\delta D_{90}/D_{90}$ ranges from 0·094 to 0·104. Uncertainty bars for the observed values of D_{90} are reported in Table II and shown in Figure 2c.

The fractional uncertainty in the GS conductance coefficient k_S is estimated using the relationship

$$\frac{\delta k_S}{k_S} = \frac{\delta Q}{Q} + \frac{1}{2}\frac{\delta S_w}{S_w} + \frac{5}{3}\frac{\delta \Omega}{\Omega} + \frac{2}{3}\frac{\delta W}{W} \tag{18}$$

Over the 12 cross-sections surveyed, $\delta k_S/k_S$ ranges from 0·166 to 0·372. Uncertainty bars for the estimated values of k_S are reported in Table II and shown in Figure 3c.

The uncertainty in the upstream drainage area A contributing to each cross-section was estimated by repeating the graphical construction of the corresponding watershed line several times. For each cross-section, the best estimate of A was assumed to be the average of the measurements obtained and the uncertainty δA was estimated to be the RMS deviation of the measurements. Cartographic reproduction errors were not considered in this study. Over the 12 cross-sections surveyed, $\delta A/A$ ranges from 0·012 to 0·022. Uncertainty bars for the computed values of A are reported in Table II and shown in Figure 3.

DATA ANALYSIS

Weighted least-squares fitting to logarithmically transformed (base 10) variables has been applied to identify possible interrelationships between observed variables. Simple power function relationships of the kind $Y = AX^B$ are assumed to connect control variables X and response variables Y, and weighted least-square fits of logarithmically transformed (base 10) observed data $x_i = \log X_i$ and $y_i = \log Y_i$ to the straight lines $y = a + bx$, where $y = \log Y$, $a = \log A$, $b = B$, and $x = \log X$, are used to evaluate these assumptions. (Note that in this paper the same symbol A is used to denote both the upstream drainage area and the coefficient in $Y = AX^B$, and the same symbol y is used to denote both the exponent in Equation (9) and the dependent variable in $y = a + bx$.) As reported by Taylor (1997: 198), constants a and b can be calculated (Appendix A) by weighting each data point (x_i, y_i) by the quantity $1/\sigma_i^2$, σ_i being the equivalent uncertainty along the y axis that may be associated to a data point (x_i, y_i) affected by uncertainty along both x and y axes. As reported by Taylor (1997: 190), this equivalent uncertainty can be calculated as

$$\sigma_i = \sqrt{\sigma_y^2 + (b\sigma_x)^2} \tag{19}$$

where σ_x and σ_y are the uncertainties along the x and y axes, respectively. Note that, for instance, the symbol σ_x denoting the standard deviation of x is adopted here to mean exactly what has been called uncertainty δx in the 'Analysis of uncertainties in field-derived data' section, on the strength of the statistical analysis of uncertainties (Taylor, 1997: 101). The values of σ_x and σ_y can be calculated as $\sigma_x = [\log(X + \sigma_X) - \log(X - \sigma_X)]/2$ and $\sigma_y = [\log(Y + \sigma_Y) - \log(Y - \sigma_Y)]/2$, where the uncertainties σ_X $(= \delta X)$ and σ_Y $(= \delta Y)$ in the variables X and Y are estimated using the concepts described in the 'Analysis of uncertainties in field-derived data' section.

Uncertainties σ_a and σ_b in the estimated constants a and b can be calculated (Appendix A) and the uncertainty intervals for coefficient A and exponent B can, therefore, be provided as $(10^{a-\sigma_a}, 10^{a+\sigma_a})$ and $(b - \sigma_b, b + \sigma_b)$ respectively. Weights $1/\sigma_i^2$ with σ_i given by Equation (19) can then be used to calculate (Appendix A) the correlation coefficient R and its quantitative significance. The quantitative significance of the correlation coefficient R is determined by evaluating a p-value that represents the probability that two uncorrelated variables (x and y) would give a coefficient R greater than or equal to the observed one (i.e. that given by Equation (A.6) in Appendix A). If this p-value is small, then it is unlikely that the two variables are uncorrelated. Correlations can therefore be called 'not significant' (NS), 'significant' (S), or 'highly significant' (HS), when $p > 0.05$, $0.01 \leq p \leq 0.05$, or $p < 0.01$ respectively (e.g. Taylor, 1997: 218). The potential influence of leverage (i.e. the potential of data points with explanatory variable values far from the average of the explanatory variable values in the entire data set to affect the model parameter estimates (e.g. Ramsey and Shafer, 2002: 316)) is not evaluated in the present study.

A first analysis is aimed to evaluate the dependence of mean flow velocity U on the factors that are commonly used in hydraulic and geomorphologic relationships, namely hydraulic depth Y_m, water-surface slope S_w (in preference to channel bed slope S_b), bed material particle size D_{90}, and upstream drainage area A. As shown in Figure 2 and reported in Table III, field-derived results support simple power function

Table III. Characteristics of power function relationships between mean flow velocity and relevant explicative variables[a]

Variable	Coefficient	Exponent	R	p-value	Significance
Y_m (Figure 2a)	0·196 (0·152, 0·252)	−0·364 (−0·522, −0·177)	−0·186	0·562	NS
S_w (Figure 2b)	0·053 (0·039, 0·070)	−0·641 (−0·740, −0·542)	−0·695	0·012	S
D_{90} (Figure 2c)	0·187 (0·172, 0·203)	−0·935 (−1·055, −0·815)	−0·863	0·001	HS
A (Figure 2d)	0·040 (0·031, 0·051)	0·887 (0·780, 0·994)	0·777	0·004	HS

[a] Values in parentheses express the uncertainty in the estimated coefficients and exponents. The p-value and the significance of R are determined by applying the methodology reported by Taylor (1997: 218).

relationships between U and S_w in a significant manner ($R = -0{\cdot}695$ with $p = 0{\cdot}012$), between U and D_{90} and between U and A in a highly significant manner ($R = -0{\cdot}863$ with $p = 0{\cdot}001$ and $R = 0{\cdot}777$ with $p = 0{\cdot}004$ respectively), whereas they do not support the relationship between U and Y_m in a significant manner ($R = -0{\cdot}186$ with $p = 0{\cdot}562$).

A second analysis is aimed at evaluating the relationship between relevant flow characteristics and upstream drainage area contributing to each stream channel cross-section surveyed. As shown in Figure 3 and reported in Table IV, field-derived results support simple power function relationships between Y_m, S_w (for S_f), k_S and A in a highly significant manner ($R = -0{\cdot}830$ with $p = 0{\cdot}002$, $R = -0{\cdot}752$ with $p = 0{\cdot}006$, and $R = 0{\cdot}929$ with $p = 0{\cdot}000$ respectively), whereas they support simple power function relationships between Q and A in a significant manner ($R = 0{\cdot}670$ with $p = 0{\cdot}019$). One can note that values of r and y reported in Table IV do not exactly verify the relationships $r = k/(c^{2/3}t^{1/2})$ and $y = m - 2/3f - 1/2z$ mentioned in the 'Study area and field campaign' section. Slight inequalities are purely connected to the application of weighted least-squares fitting (with variable weights).

A third analysis is finally aimed at evaluating predictions of mean flow velocity along the stream monitored. Four mathematical formulations are considered: (a) the DW Equation (1) with f given by Equations (3) and (4), (b) the GMS Equation (2) with k_S given by Equation (5), (c) the U–A fluvial relationship in Equation (6) with parameters reported in Table III, and (d) the GMS Equation (2) with k_S and Y_m given by Equations (9) and (7) respectively, and parameters reported in Table IV. Calculated and measured flow velocities are compared visually in Figure 4. The mean error (ME), mean absolute error (MAE), and root-mean-square error (RMSE) between predicted ($\hat{U}_i$) and observed (U_i) velocities are calculated (Appendix B) by using weights $1/\sigma^2_{U_i}$ that account for the uncertainty in observed flow velocities U_i. Results are reported in Table V.

In Figure 4, uncertainty bars are reported for both observed flow velocities (horizontal bars) and for predicted flow velocities (vertical bars). For all the mathematical formulations (a)–(d) mentioned above, uncertainty bars in predicted flow velocities are calculated by propagating uncertainties in the control variables through sums in quadrature (Taylor, 1997: 75). For instance, the uncertainties in flow velocities U provided by

Table IV. Characteristics of power function relationships between relevant hydraulic quantities and upstream drainage area[a]

Variable	Coefficient	Exponent	R	p-value	Significance
Y_m (Figure 3a)	0·739 (0·708, 0·771)	−0·422 (−0·440, −0·403)	−0·830	0·002	HS
S_f (Figure 3b)	0·861 (0·667, 1·111)	−1·125 (−1·225, −1·024)	−0·752	0·006	HS
k_S (Figure 3c)	0·054 (0·034, 0·087)	1·744 (1·551, 1·936)	0·929	0·000	HS
Q (Figure 3d)	0·021 (0·017, 0·026)	1·312 (1·231, 1·393)	0·670	0·019	S

[a] Values in parentheses express the uncertainty in the estimated coefficients and exponents. The p-value and the significance of R are determined by applying the methodology reported by Taylor (1997: 218).

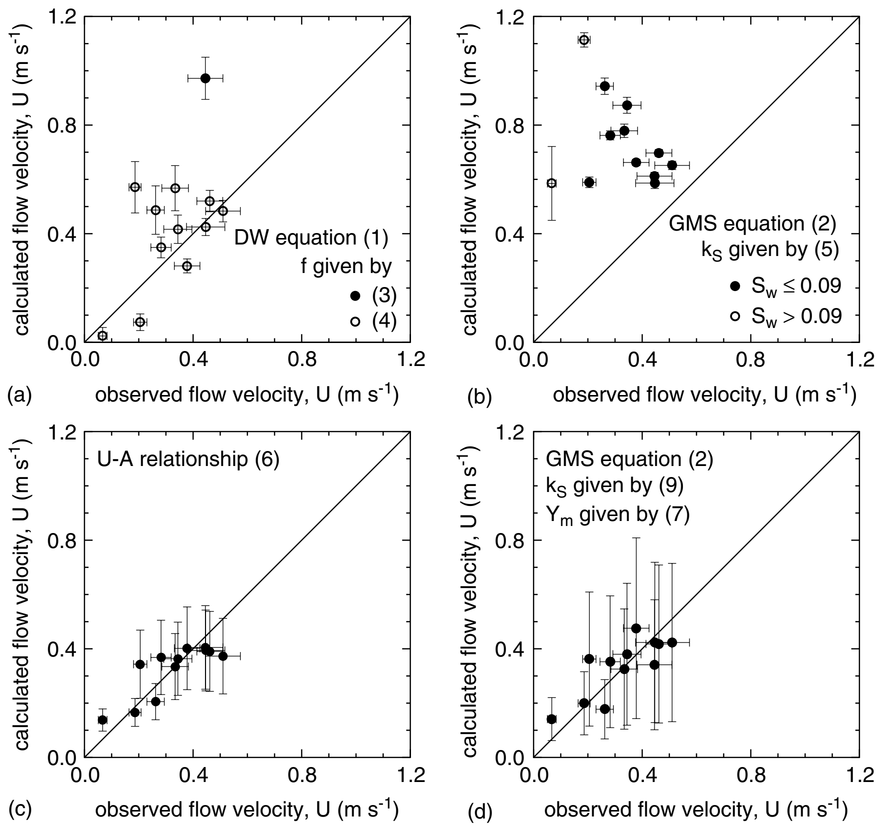

Figure 4. Comparison between measured and calculated flow velocities (Table V)

Table V. Errors between measured and calculated flow velocities

Mathematical formulation	ME (m s^{-1})	MAE (m s^{-1})	RMSE (m s^{-1})
DW Equation (1) and relationships in Equations (3) and (4) (Figure 4a)	0·106	0·161	0·218
GMS Equation (2) and relationship in Equation (5) (Figure 4b)	0·412	0·412	0·477
U–A fluvial relationship in Equation (6) (Figure 4c)	−0·010	0·063	0·077
GMS Equation (2) and relationships in Equations (9) and (7) (Figure 4d)	0·005	0·068	0·081

Equations (1) and (4), where S_w is used to approximate both S_f and S_b, are calculated by means of

$$\delta U = \sqrt{\left(\frac{\partial U}{\partial Y_m}\delta Y_m\right)^2 + \left(\frac{\partial U}{\partial S_w}\delta S_w\right)^2 + \left(\frac{\partial U}{\partial f}\delta f\right)^2} \tag{20}$$

and

$$\delta f = \sqrt{\left(\frac{\partial f}{\partial Y_m}\delta Y_m\right)^2 + \left(\frac{\partial f}{\partial D_{90}}\delta D_{90}\right)^2 + \left(\frac{\partial f}{\partial S_w}\delta S_w\right)^2} \tag{21}$$

The results are reported in Table VI.

Table VI. Uncertainties in flow velocities calculated using the mathematical formulations (a)–(d) mentioned in the 'Data analysis' section

XS	δU (m s^{-1})			
	(a)	(b)	(c)	(d)
1	0·031	0·136	0·041	0·079
2	0·095	0·026	0·051	0·116
3	0·089	0·030	0·067	0·109
4	0·083	0·025	0·122	0·222
5	0·031	0·020	0·126	0·247
6	0·052	0·029	0·135	0·261
7	0·038	0·017	0·137	0·243
8	0·040	0·015	0·139	0·292
9	0·039	0·013	0·147	0·291
10	0·031	0·020	0·149	0·295
11	0·026	0·012	0·152	0·333
12	0·078	0·014	0·154	0·239

DISCUSSION

First of all, it is acknowledged that the field data reported in this paper were collected at a small number (12) of cross-sections (Table I) along a portion of the Febbraro catchment mainstem (Figure 1); therefore, their representativity must be qualified accordingly. However, it is also remarked that the high accuracy with which surveys were conducted and uncertainties were estimated may hardly be exercised in extensive field campaigns. Field surveys and data analysis methods presented in this paper are designed to provide a circumscribed but very accurate inspection. This approach is relevant to characterizing a mountain stream using a small number of cross-sections surveyed and, perhaps more importantly, to providing useful guidelines for future (more extensive) investigative efforts.

Using the data collected along the Febbraro River, the hydraulic relationship in Equation (3) is found to overestimate significantly the predicted flow velocity at cross-section 12 (Figure 4a, Table VI), whereas the hydraulic relationship in Equation (4) is found to provide reasonable predictions of mean flow velocity (Figure 4a, Tables V and VI), at least with respect to other study cases (e.g. Orlandini, 2002). This is likely to be connected to the good (negative) correlations between U and S_w, and between U and D_{90} (Figure 2b and c respectively, Table III). Using S_w to approximate S_f and S_b, and focusing the attention on the relationship in Equation (4), one can note that Equation (1) implies that $f = (8gY_mS_w)/U^2$, whereas Equation (4) implies that $f = f(Y_m, D_{90}, S_w)$. Hence, by combining the expressions of f derived from Equations (1) and (4), one can obtain the functional relationship $(8gY_mS_w)/U^2 = f(Y_m, D_{90}, S_w)$. This equation may hold only if $U = U(Y_m, D_{90}, S_w)$. From the field data shown in Figure 2a and reported in Table III, it may be observed that the dependence of U on Y_m along the Febbraro River is weak (statistically not significant; 'Data analysis' section). Therefore, it may be inferred (although in qualitative terms) that the strength of predictions shown in Figure 4a is likely to be connected to the goodness of dependencies of U upon S_w and of U on D_{90}.

Equation (5) is found to be insufficiently general to reproduce the observed variability of mean flow velocity along the Febbraro River (Figure 4b, Tables V and VI). With a reasoning similar to that reported above, from Equation (2) and the relationship in Equation (5) one can obtain the functional relationship $U/(Y_m^{2/3}S_w^{1/2}) = k_S(Y_m, S_w)$ and may infer (although in qualitative terms) that the poor predictions shown in Figure 4b are likely to be determined by the dependencies of U upon Y_m and of U on S_w (Figure 2a and b respectively, Table III). In the case examined in this paper, the insignificant dependence of U on Y_m (Figure 2a, Table III) and the low exponent with which U depends on S_w in the combined Equations (2) plus (5) (i.e. $U = 3{\cdot}125Y_m^{0{\cdot}83}S_f^{0{\cdot}12}$, S_f being approximated by S_w) are likely to be responsible of the poor agreement between predicted and observed values of mean flow velocity. The relationships in Equations (3), (4), and (5) need not be calibrated using observed data, but they may produce significant bias and dispersion in predicted flow velocities (Figure 4a and b, Tables V and VI).

To reduce the bias and dispersion in predicted flow velocities, fluvial relationships of the upstream drainage area can be estimated using observed data. At least when uncertainties in relevant variables have comparable magnitude, if a relationship exists between U and S_w, a relationship between U and A can be expected to come out since a relationship between S_w and A is commonly observed in nature (Leopold and Maddock, 1953). In the case examined in this paper, U is satisfactorily related to A (Figure 2d, Table III) and Equation (6), with k and m reported in Table III, may be used to predict mean flow velocity along the Febbraro River (Figure 4c, Tables V and VI). It is first specified that the sharp downstream increase in mean flow velocity reported in this study should not be compared with variations observed along low-gradient rivers during bankfull conditions, but rather with variations observed in high-gradient streams during low-flow conditions (Bathurst, 1993: 94; Leopold, 1997: 56; Orlandini, 2002). Second, it is noted that an anomalous decrease of hydraulic depth is observed along the fluvial system surveyed (Figure 3a, Table IV) and, in this specific case, the downstream increase of mean flow velocity cannot be connected to the downstream increase of hydraulic depth as reported by Leopold (1997: 56), but to some (unknown) more general principle underlying the hydraulic functioning of mountain streams. Third, it is remarked that, although significant deviations of observed flow discharges from a power function relationship of the upstream drainage area occur along the Febbraro River (Figure 3d, Table IV), cross-sectional flow areas appear to respond to these deviations so as to allow a more regular variation of U with A (Figure 2d, Table III).

A more detailed analysis of the spatial variation of resistance to flow along the Febbraro River can be performed by considering the relative role that the spatial variation (with A) of each flow characteristic included in the right-hand side of Equation (11) plays in the determination of the spatial variation (with A) of the GS conductance coefficient. The downstream increase in k_S (Figure 3c, Table IV) is found to be determined by the sharp downstream increase in U (Figure 2d, Table III) and by the anomalous downstream decrease in Y_m (Figure 3a, Table IV) discussed above, as well as by the expected downstream decrease in S_w used to approximate the downstream decrease in S_f (Figure 3b, Table IV). In this respect, simple fluvial relationships allow one to incorporate the essential spatial variability of flow characteristics along a complex mountain stream during quasi-steady, low-flow conditions and to provide accurate predictions of U as functions of A and S_w (Figure 4d, Tables V and VI). However, it must also be noted that the use of fluvial relationships of A for k_S and Y_m instead of direct measurements produces large uncertainty bars (vertical bars) in predicted flow velocities (Figure 4d, Table VI). Reducing these uncertainty bars, therefore, depends upon improving the characterizations for the spatial variations (with A) of k_S and Y_m. This emphasizes the limitations of field data collected during quasi-steady, low-flow conditions and the expected advantages offered by field data collected at the bankfull stage.

CONCLUSIONS

The analysis carried out in this paper suggests the following conclusions. A strong dependence of U on S_w and D_{90} (Figure 2b and c, Table III) may allow hydraulic Equations (4) and (1) to provide reasonable DW resistance coefficients f and predictions of mean flow velocity U along a mountain stream (Figure 4a, Tables V and VI). An anomalous dependence of U on Y_m (Figure 2a, Table III) may cause the hydraulic relationships in Equations (5) and (2) to provide inaccurate GS conductance coefficients k_S and to not reproduce the observed spatial variability of mean flow velocity U along the stream (Figure 4b, Tables V and VI). When U is strongly negatively correlated with S_w (Figure 2b, Table III) and S_w is strongly negatively correlated with A (Figure 3b, Table IV), a good geomorphological relationship between U and A may be estimated (Figure 2d, Table III) to improve significantly the predictions of U with respect to those provided by hydraulic formulations (Figure 4c, Tables V and VI). The combined use of both the explicative variables A and S_w outlined in the 'Background' section slightly reduces the bias and increases the dispersion in the predictions of U with respect to the application of the U–A fluvial relationship alone (Figure 4d, Tables V and VI) and, more importantly, allows a useful characterization of the GS conductance coefficient k_S along a steep Alpine stream (Figure 3c, Table IV). The field data and analysis presented in this study reveal that resistance to flow along the Febbraro River decreases (i.e. k_S increases, Figure 3c, Table IV) downstream rapidly enough for flow velocity to increase (Figure 2d, Table III), despite the expected decrease in water-surface slope (Figure 3b, Table IV) and the unexpected decrease in hydraulic depth (Figure 3a, Table IV). This may be attributable, at least in part, to the downstream decrease in bed material particle size (Table I) and, more generally, to the controls that climate and geology have on channel morphology. Future work is promoted to investigate these complex relationships.

ACKNOWLEDGEMENTS

This research was jointly supported by the Gruppo Nazionale per la Difesa dalle Catastrofi Idrogeologiche (grant 03.00042.GN42, Rome, Italy) and by the Istituto Nazionale per la Ricerca Scientifica e Tecnologica sulla Montagna (grant 378/02, Rome, Italy). We thank Claudio Paniconi (INRS-ETE, University of Quebec, Quebec city, Canada), Stephen Lancaster and John Faustini (Oregon State University, Corvallis, USA), and an anonymous reviewer for comments that led to improvements in the manuscript.

APPENDIX A: WEIGHTED FIT FOR A STRAIGHT LINE

If data points (x_i, y_i) are expected to lie on a straight line $y = a + bx$ and if the measurements of x_i and y_i have estimated equivalent uncertainty σ_i in y_i given by Equation (19), then the weights

$$w_i = 1/\sigma_i^2 \tag{A.1}$$

can be introduced and the best estimates for the constants a and b can be calculated as

$$a = \frac{\sum w_i x_i^2 \sum w_i y_i - \sum w_i x_i \sum w_i x_i y_i}{\sum w_i \sum w_i x_i^2 - \left(\sum w_i x_i\right)^2} \tag{A.2}$$

and

$$b = \frac{\sum w_i \sum w_i x_i y_i - \sum w_i x_i \sum w_i y_i}{\sum w_i \sum w_i x_i^2 - \left(\sum w_i x_i\right)^2} \tag{A.3}$$

The solution of Equations (19), (A.1), (A.2), and (A.3) can readily be obtained by implementing a simple iterative procedure. Uncertainties in the calculated constants a and b are given by

$$\sigma_a = \sqrt{\frac{\sum w_i x_i^2}{\sum w_i \sum w_i x_i^2 - \left(\sum w_i x_i\right)^2}} \tag{A.4}$$

and

$$\sigma_b = \sqrt{\frac{\sum w_i}{\sum w_i \sum w_i x_i^2 - \left(\sum w_i x_i\right)^2}} \tag{A.5}$$

The correlation coefficient is given by

$$R = \frac{\sum w_i(x_i - \overline{x})(y_i - \overline{y})}{\sqrt{\sum w_i(x_i - \overline{x})^2 \sum w_i(y_i - \overline{y})^2}} \tag{A.6}$$

where weighted averages $\overline{x} = \sum w_i x_i / \sum w_i$ and $\overline{y} = \sum w_i y_i / \sum w_i$ must be used.

APPENDIX B: MEAN ERRORS

ME, MAE, and RMSE between predicted velocity $\hat{U}_i$ and observed velocity U_i are calculated as

$$\mathrm{ME} = \frac{\sum w_i(\hat{U}_i - U_i)}{\sum w_i} \tag{B.1}$$

$$\mathrm{MAE} = \frac{\sum w_i|\hat{U}_i - U_i|}{\sum w_i} \tag{B.2}$$

and

$$\mathrm{RMSE} = \sqrt{\frac{\sum w_i(\hat{U}_i - U_i)^2}{\sum w_i}} \tag{B.3}$$

where weights $w_i = 1/\sigma^2_{U_i}$ account for the uncertainty in observed flow velocities.

REFERENCES

Barnes HH. 1967. Roughness characteristics of natural channels. *US Geological Survey Water Supply Paper* 1849.

Bathurst JC. 1985. Flow resistance estimation in mountain rivers. *Journal of Hydraulic Engineering, ASCE* **111**: 625–643.

Bathurst JC. 1993. Flow resistance through the channel network. In *Channel Network Hydrology*, Beven K, Kirkby MJ (eds). Wiley: New York; 69–98.

Graf WH, Cao HH, Suszka L. 1983. Hydraulics of steep, mobile-bed channels. In *20th Conference of the International Association of Hydraulics Research*, vol. 7, Moscow; 301–305.

Hager WH. 2001. Gauckler and the GMS formula. *Journal of Hydraulic Engineering, ASCE* **127**: 635–638.

Hicks DM, Mason P. 1991. *Roughness characteristics of New Zealand rivers*. Water Resources Survey, DSIR Marine and Freshwater, Wellington, New Zealand.

Jacobson RB, Femmer SR, McKenney RA. 2001. *Land-use changes and physical habitat of streams: a review with emphasis on studies within the U.S. Geological Survey Federal-State cooperative program*. US Geological Survey Circular 1175.

Jarrett RD. 1984. Hydraulics of high-gradient streams. *Journal of Hydraulic Engineering, ASCE* **110**: 1519–1539.

Leopold LB. 1997. *Water, Rivers and Creeks*. University Science Books: Sausalito, CA.

Leopold LB, Maddock Jr T. 1953. The hydraulic geometry of stream channels and some physiographic implications. *US Geological Survey Professional Paper* 252.

Leopold LB, Wolman MG, Miller JP. 1964. *Fluvial Processes in Geomorphology*. W. H. Freeman: San Francisco, CA.

MacFarlane WA, Wohl E. 2003. Influence of step composition on step geometry and flow resistance in step–pool streams of the Washington Cascades. *Water Resources Research* **39**: 1037. DOI: 10·1029/2001WR001238.

Nolan KM, Shields RR. 2000. *Measurement of stream discharge by wading*. US Geological Survey Water Resources Investigation Report 00–4036.

Orlandini S. 2002. On the spatial variation of resistance to flow in upland channel networks. *Water Resources Research* **38**: 1197. DOI: 10·1029/2001WR001187.

Orlandini S, Rosso R. 1998. Parameterization of stream channel geometry in the distributed modeling of catchment dynamics. *Water Resources Research* **34**: 1971–1985.

Ramsey FL, Shafer DW. 2002. *The Statistical Sleuth: A Course in Methods of Data Analysis*. Duxbury: Pacific Grove, CA.

Smart GM, Jaeggi MNR. 1983. *Sediment transport on steep slopes*. Mitteilungen der Versuchsanstalt für Wasserbau, Hydrologie und Glaziologie, No. 64. Eidgenössische Technische Hochschule, Zürich, Switzerland (in German).

Taylor JR. 1997. *An Introduction to Error Analysis: The Study of Uncertainties in Physical Measurements*. University Science Books: Sausalito, CA.

Williams GP. 1970. Manning formula: a misnomer? *Journal of Hydraulics Division, ASCE* **96**: 193–200.

Wohl EE. 2000. *Mountain Rivers*. Water Resources Monograph 14. American Geophysical Union: Washington, DC.

Wolman MG. 1954. A method of sampling coarse river-bed material. *Eos, Transactions of the American Geophysical Union* **35**: 951–956.